IEEE CSC & ESAS SUPERCONDUCTIVITY NEWS FORUM (global edition), No. 49, March 2021.
Invited presentation Wk2EOr4A-04 given at the virtual ASC 2020, November 5, 2020.

Simulating Loss in Superconducting Qubits

Conal E. Murray (conal@us.ibm.com)
IBM T.J. Watson Research Center, Yorktown Heights, NY

ASC 2020: QE2 - Quantum Engineering & its Applications for Computing & Networks
November 5, 2020

IEEE CSC & ESAS SUPERCONDUCTIVITY NEWS FORUM (global edition), No. 49, March 2021.
Invited presentation Wk2EOr4A-04 given at the virtual ASC 2020, November 5, 2020.

Outline

- Quantum computing
  - superconducting transmon qubit
- Performance limitations
  - loss mechanisms
- Predicting dielectric loss in qubit designs
  - analytical vs. FEM approaches
- Implications for quantum computing

IBM **Quantum**

Scaling in conventional computing

- lithography is no longer sufficient in improving device performance

- new materials and new geometries enable continued scaling:
  - ➢ High-K dielectric gate oxides
  - ➢ $Si_{1-x}Ge_x$ source / drain / channel regions
  - ➢ 3D transistors

- fighting Boltzmann tyranny: $$\frac{\Delta V_{\mathrm{min}}}{\mathrm{decade}} \sim \frac{k_B T}{e} \ln(10)$$

- new computing paradigms are emerging

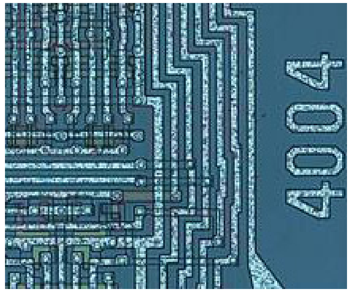

wall321.com

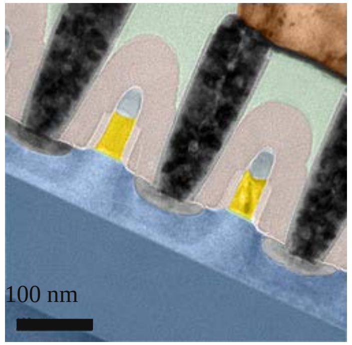

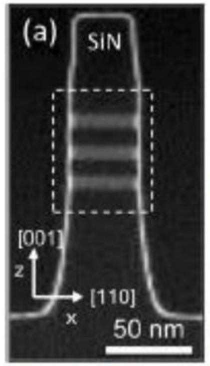

G. Tsutsui et al., AIP Advances 9, 030701 (2019)

IEEE CSC & ESAS SUPERCONDUCTIVITY NEWS FORUM (global edition), No. 49, March 2021.
Invited presentation Wk2EOr4A-04 given at the virtual ASC 2020, November 5, 2020.

Computing with qubits

Classical bits

0

1

- ✘ superposition ✓
- ✘ entanglement ✓

Quantum bits

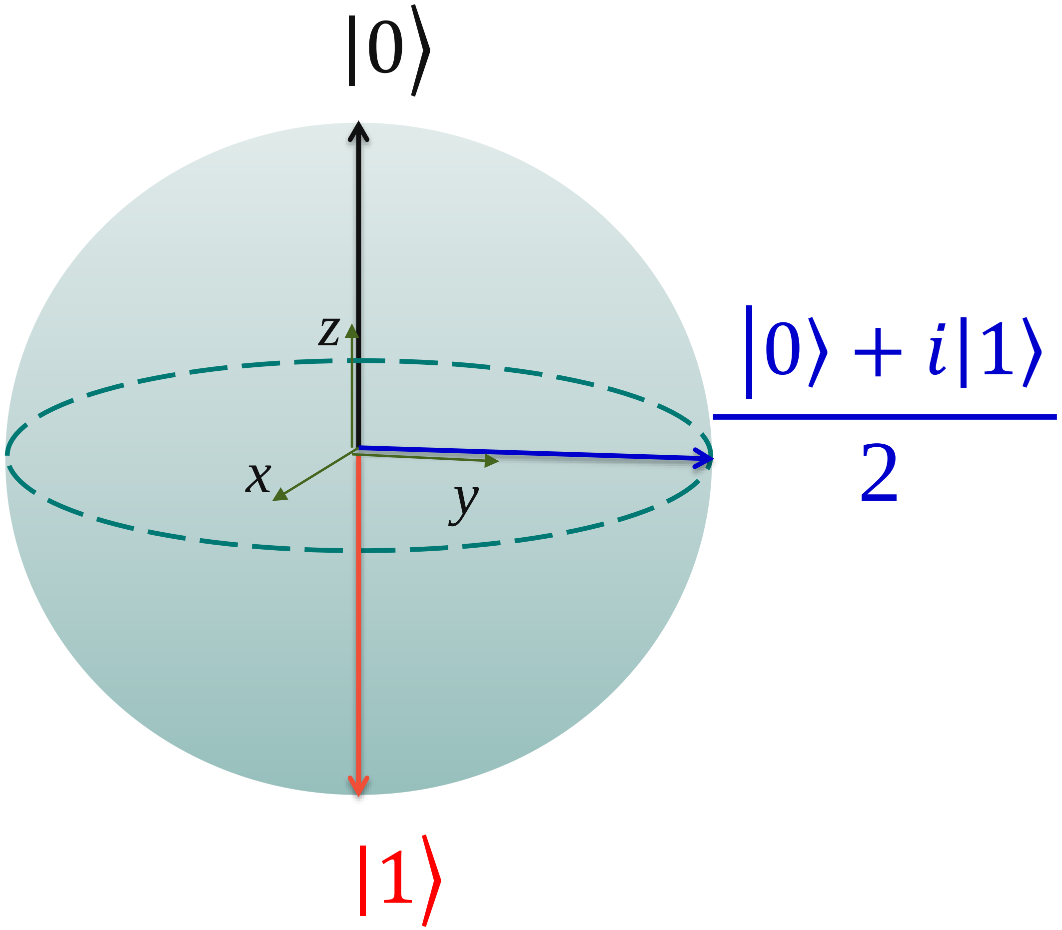

Ions

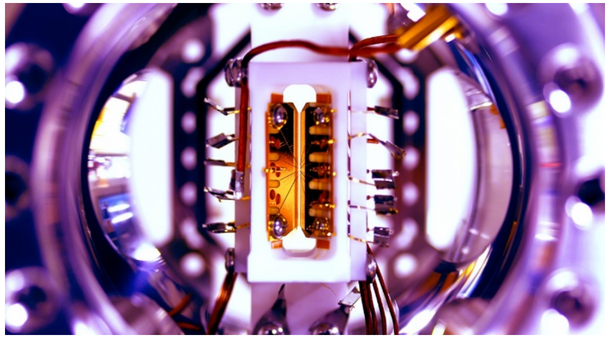

Credit: S. Debnath and E. Edwards/JQI
Monroe Group, University of Maryland/JQI

Photons

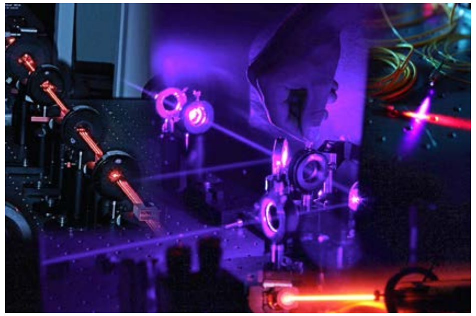

Image from the Centre for Quantum Computation & Communication Technology, credit Matthew Broome

Nanowires

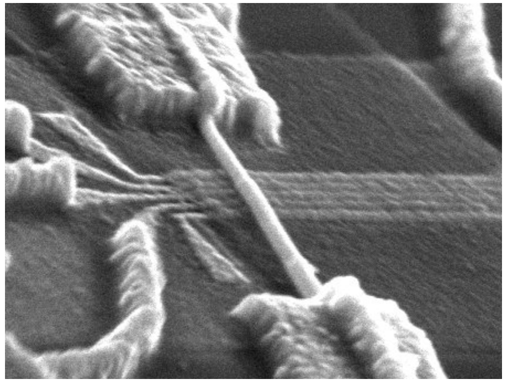

Image from Kouwenhoven Group, Delft

Quantum Computing Technologies

Solid-state defects

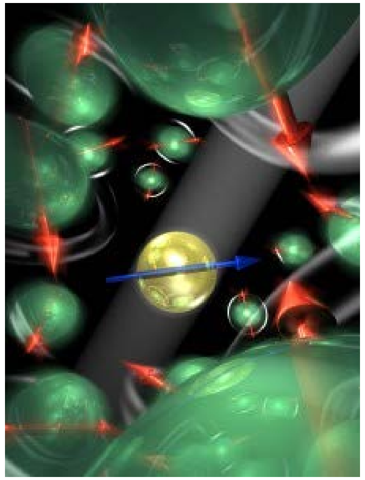

NV Centers, Phosphorous in Si, SiC defects, etc.

Image from Hanson Group, Delft

Neutral Atoms

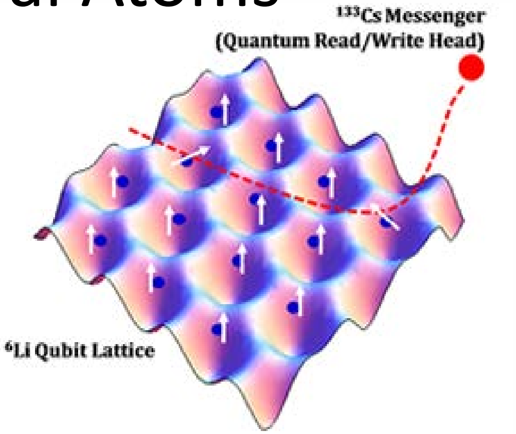

Image from Cheng Group, University of Chicago

Superconducting Circuits

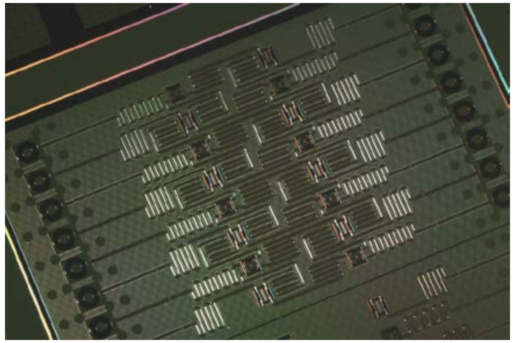

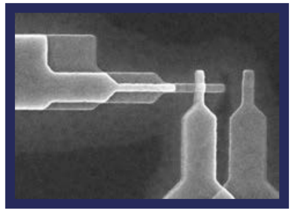

IBM **Quantum**

Anatomy of a Superconducting Qubit: Transmon

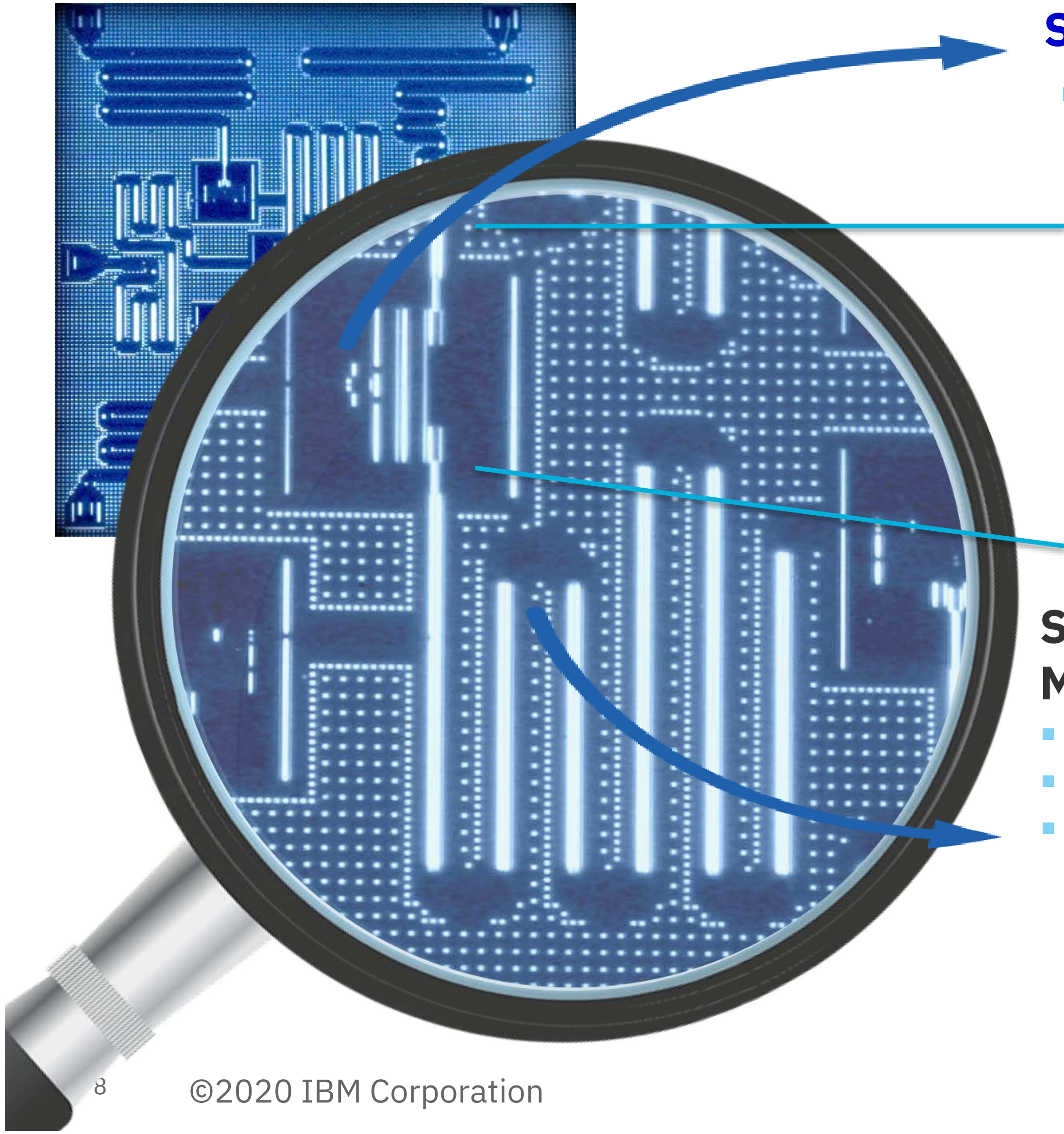

Superconducting Qubit:

- Josephson Junction as a non-linear inductor

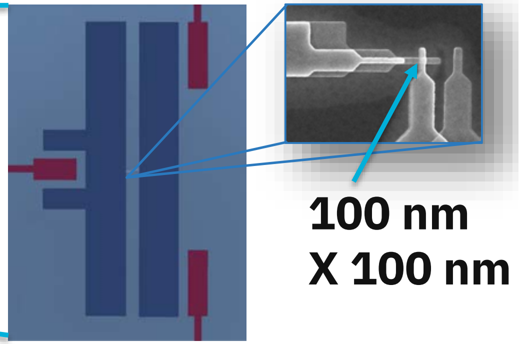

JJ-C Oscillator: *anharmonic*
→ individual transitions addressable

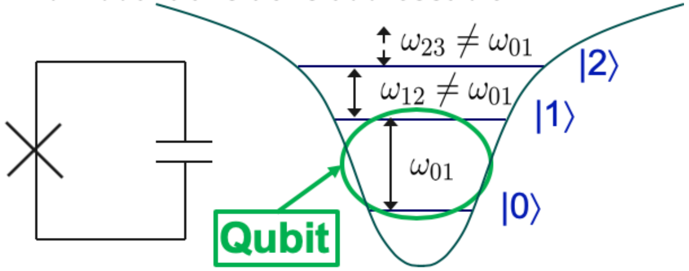

Anharmonicity = ω_{01} - ω_{12}

Superconducting Microwave Resonators:

- read-out of qubit states
- multi-qubit quantum bus
- noise filter

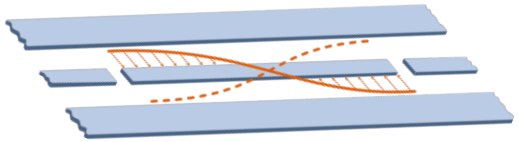

L-C Oscillator: *harmonic*
→ can't address individual transitions

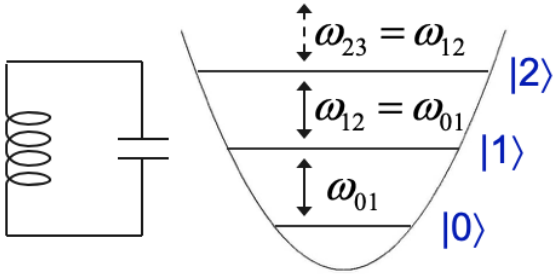

J. Koch et al., PRA **76**, 042319 (2007)

IBM **Quantum**

Evolution of Superconducting Qubit Lifetimes

- increase from nanoseconds to 100 μs over 2 decades
  - ➢ materials
  - ➢ processing
  - ➢ design
  - ➢ infrastructure

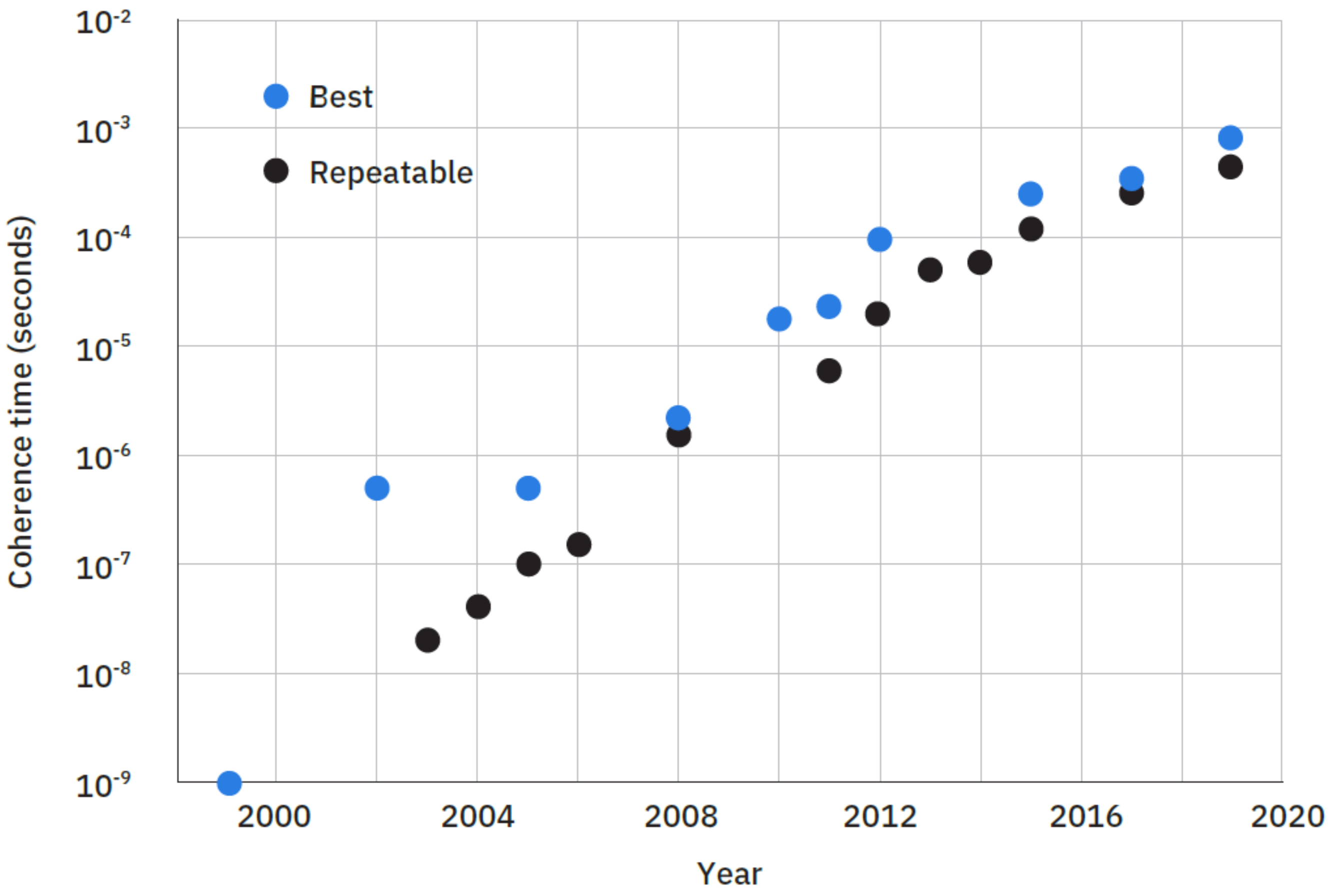

IBM **Quantum**

What mechanisms can affect qubit coherence?

- dielectric loss
- spontaneous emission (Purcell loss)
- magnetic fields
- thermalization
- parasitic modes
- others (cosmic rays?)

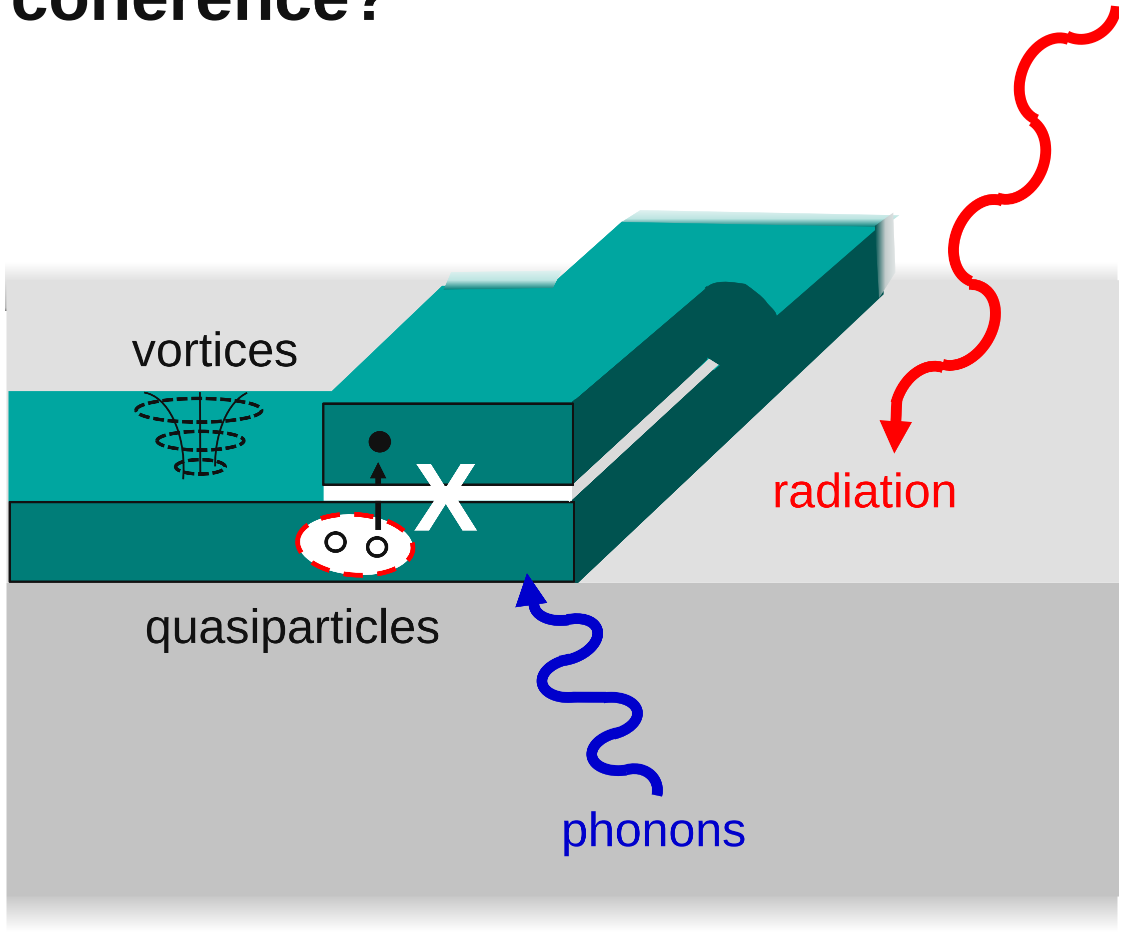

IBM **Quantum**

Dielectric loss

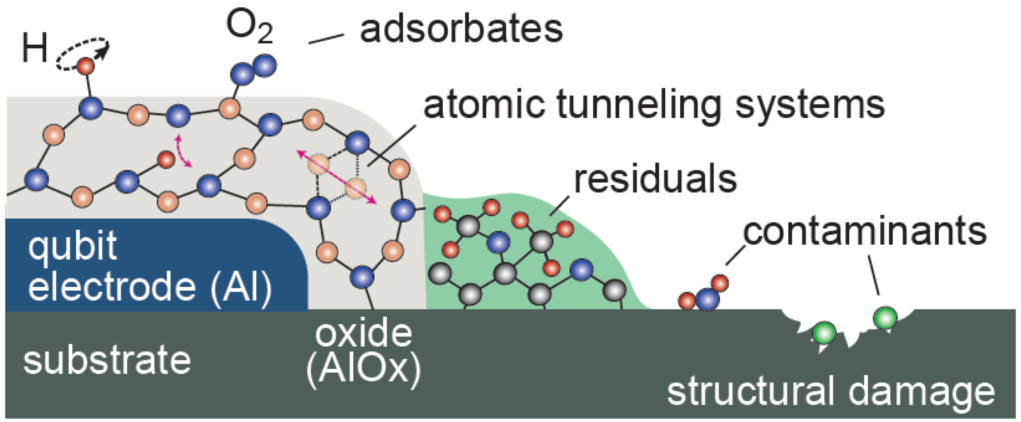

J. Lisenfeld et al., arxiv1909.09749

Two-level system (TLS)

- radiative dissipation
  - ➢ alignment of dipole frequency, moment
  - ➢ greater absorption at low power (unsaturated)

- extrinsic (contamination) vs. intrinsic behavior

- continuum approximation → $\tan(\delta) = \dfrac{\mathrm{Im}[\varepsilon]}{\mathrm{Re}[\varepsilon]}$

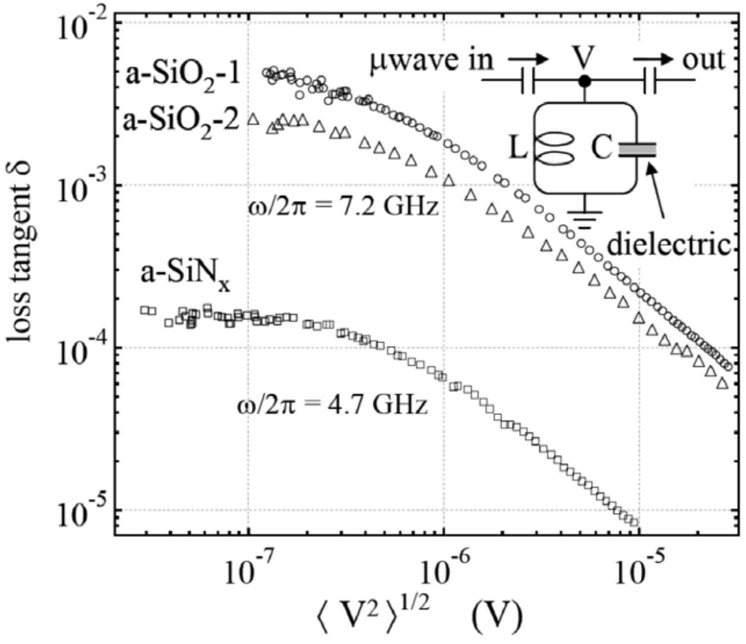

J.M. Martinis et al., PRL **95**, 210503 (2005)

IBM **Quantum**

Processing effects: CPW resonators

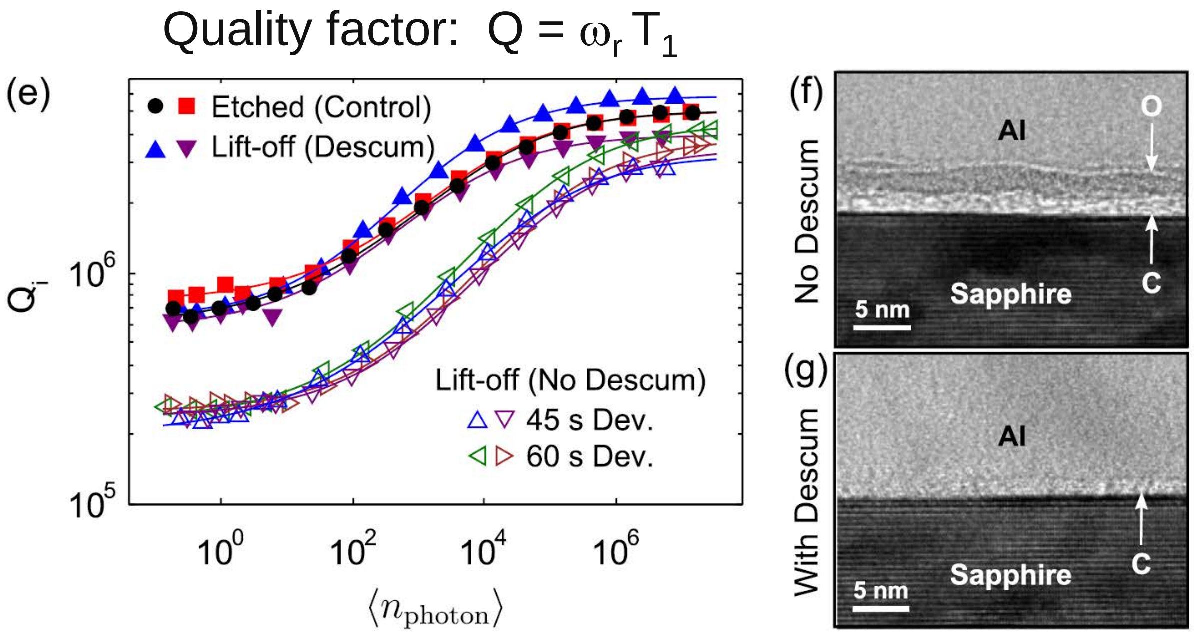

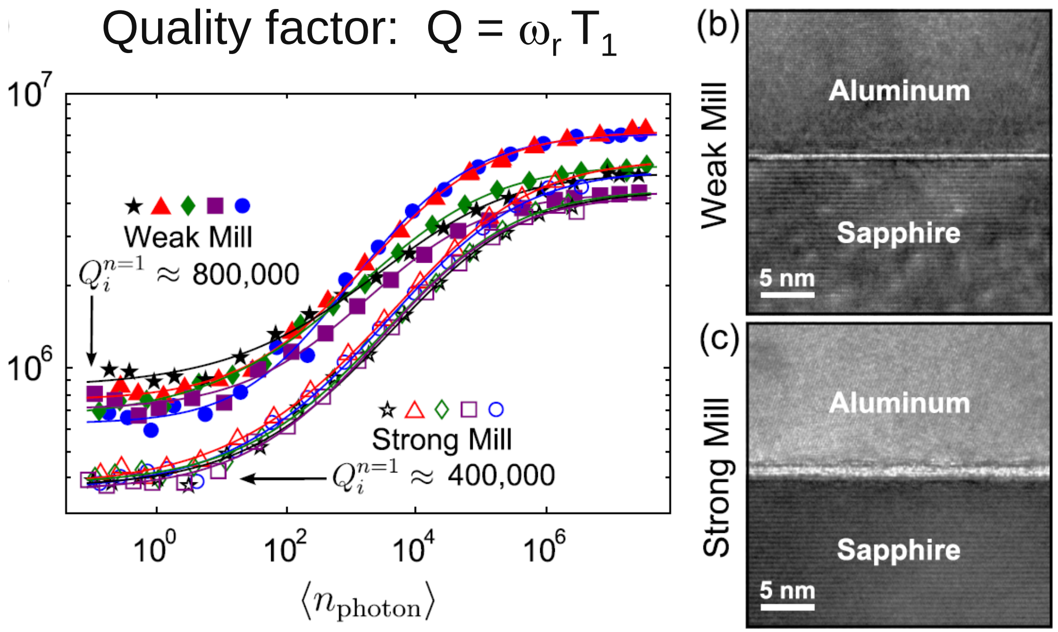

- ➢ residual contamination
- ➢ damage / amorphization due to ion milling

C.M. Quintana et al., APL **105**, 062601 (2014)

Materials matter

IBM **Quantum**

- consider qubits with interdigitated capacitors
- Al / Al_2O_3 / Al Josephson junctions
- evaporated Al vs. sputtered TiN or Nb shunting metallization
  - ➢ extrinsic or intrinsic effects ?

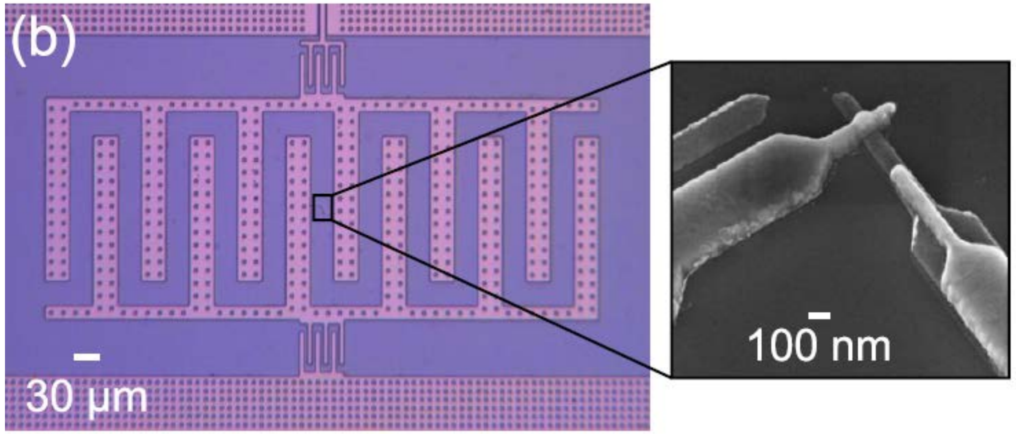

Quality factor: $Q = \omega_q T_1$

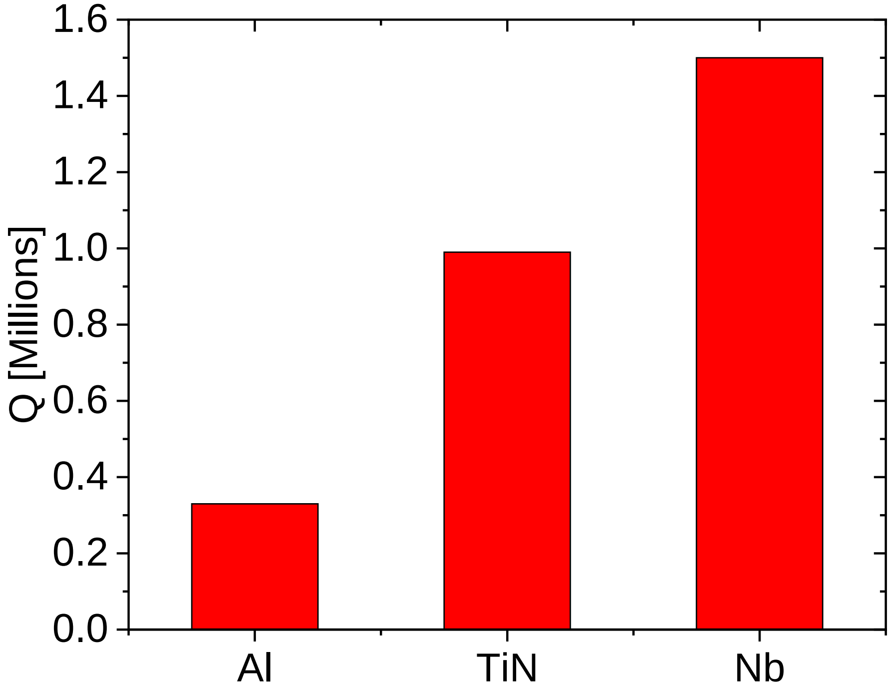

J.B. Chang et al., APL **103**, 012602 (2013)
J.M. Gambetta et al., IEEE TAS **27**, 1700205 (2017)

Evolution of Transmon Design

IBM **Quantum**

- interdigitated capacitors (IDC) → rectangular capacitors
- equivalent capacitance (proximity vs. size)
  - ➢ significant difference in electric field energy distributions

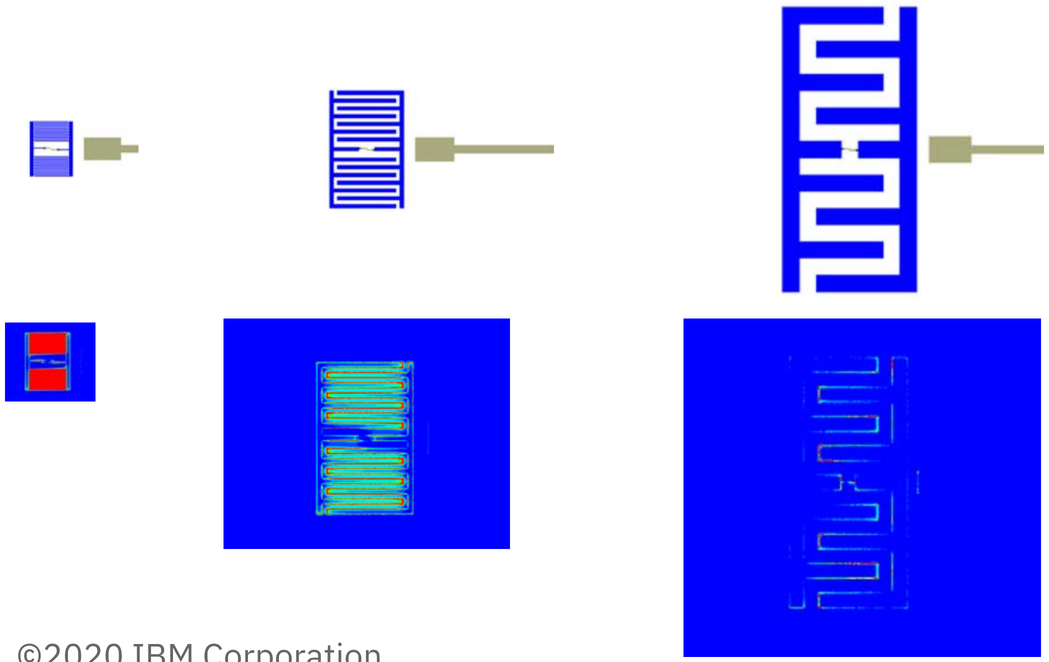

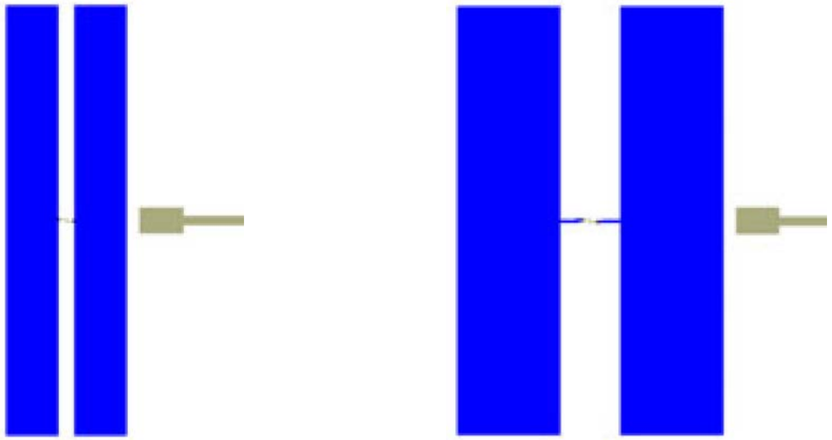

J.M. Gambetta et al., IEEE TAS **27**, 1700205 (2017)

Quantifying E-field energy

Participation: relative fraction of electric field energy, U_i / U_{tot}, within various regions

- Substrate-to-metal (SM)
- Substrate-to-air (SA)
- Metal-to-air (MA)

$$\boxed{U_i = \int_{V_i} \varepsilon_c \vec{E} \cdot \vec{E}^* dV}$$

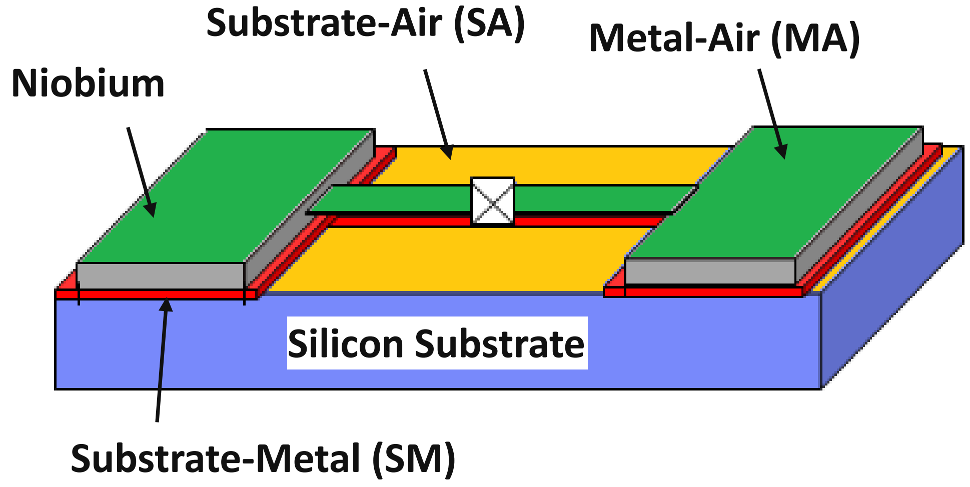

Consider thin, contamination layers:

- ➢ disparity in length scales between metallization (μm) and contamination (nm)
- ➢ singular E-field distributions near edges of metallization

IBM **Quantum**

Approximation: surface participation

- contamination layer thickness, *t*, may be unknown

➢ replace volume integral with surface integral (sheet):

$$\frac{\mathrm{P_i}}{t} \equiv p_i = \frac{\int_{S_i} \varepsilon_c \vec{E} \cdot \vec{E}\, dS}{\mathrm{U_{tot}}}$$

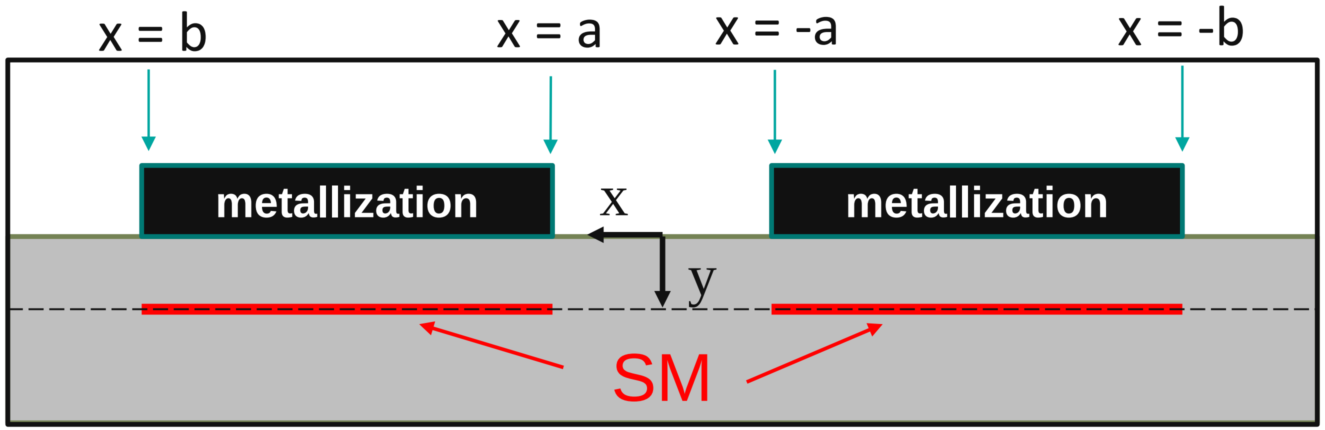

✗ assumes linear dependence with *t*

✗ singular E-fields → divergent integral at metallization bottom (y = 0)

➢ consider p_i behavior as a function of distance, y, from metallization bottom

IBM **Quantum**

Finite Element Method (FEM) solutions

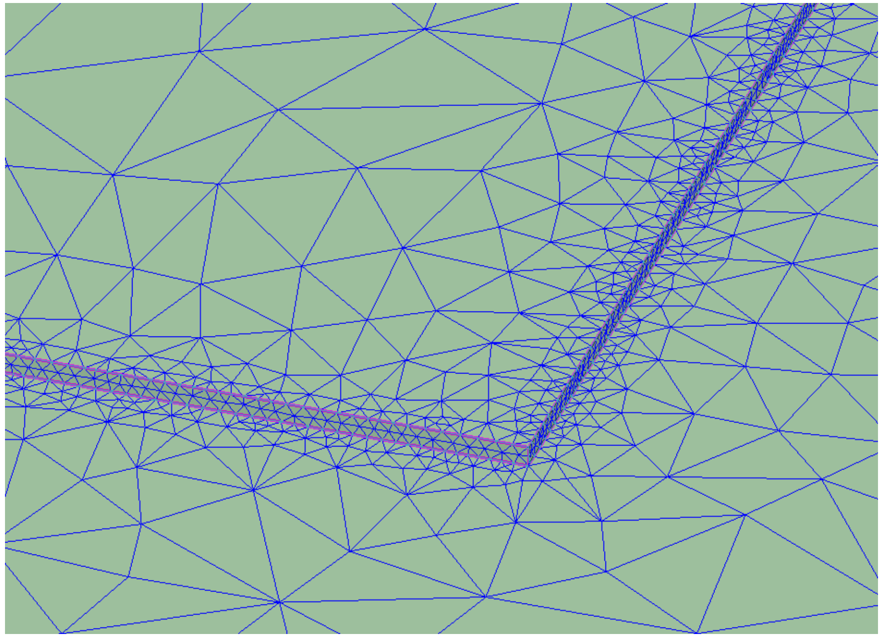

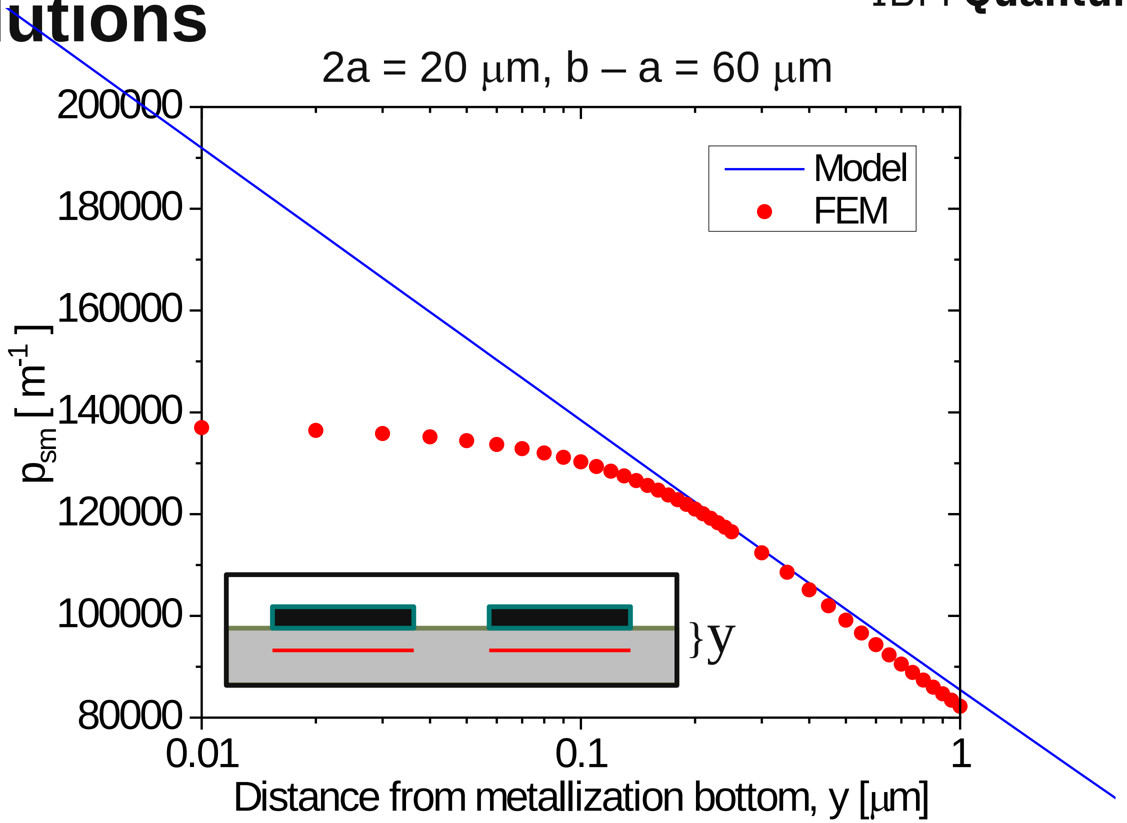

✓ versatile

✓ logarithmic dependence vs. depth

× interpolation of weak formulation

× FEM approach exhibits roll-off

➢ need analytical approach that can properly account for E-field singularities

IBM **Quantum**

Analytical modeling of (volume) participation

consider quasi-static distribution of E-fields in a 2D slice ($\nabla^2\varphi = 0$):

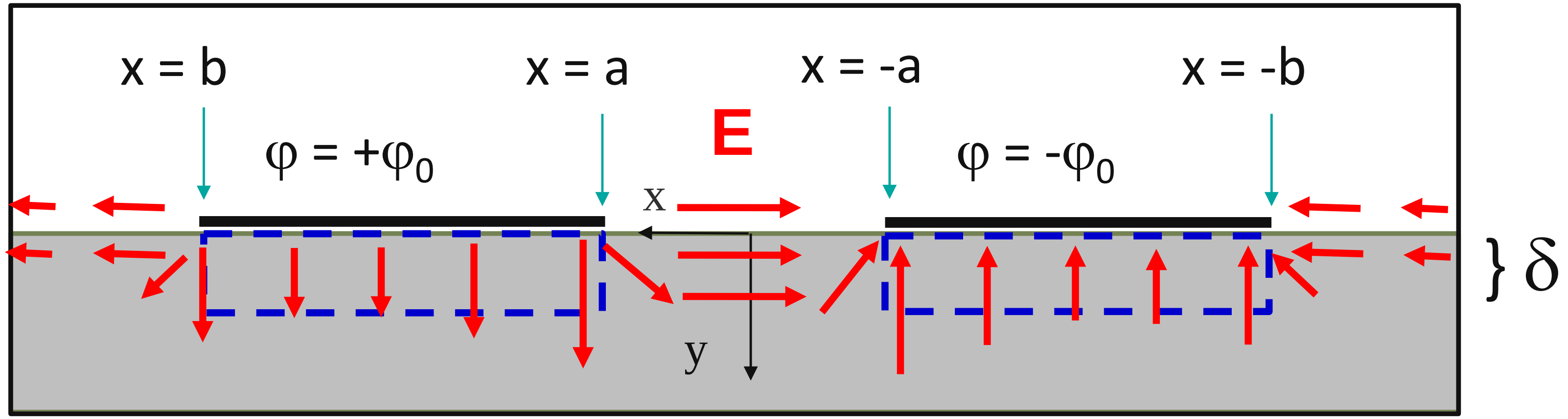

- Green's first identity (1828):

$$U_i = \int_{V_i} \varepsilon_c \nabla\varphi \cdot \nabla\varphi \, dV = \boxed{\oint_{S_i} \varepsilon_c \, \varphi(\hat{n} \cdot \nabla\varphi) \, dS} \quad \text{where} \quad \vec{E} = -\nabla\varphi$$

➢ integrate $\varphi, \hat{n} \cdot \vec{E}$ along contour

IBM **Quantum**

Solution: effect of dielectric constants (ε)

E-field boundary conditions dictated by difference in ε_i:

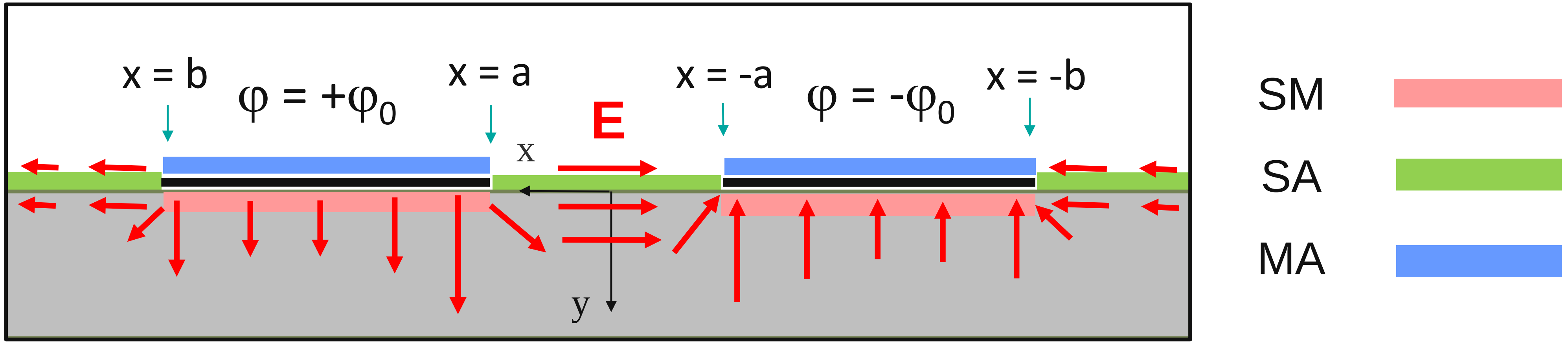

Assume all ε_c are equal:

P_{SM} / P_{SA} ~ $(\varepsilon_{sub} / \varepsilon_c)^2$ ~ 1 - 6

P_{MA} / P_{SM} ~ $(1 / \varepsilon_{sub})^2$ ~ **0.01**

$$E_1^{\parallel} = E_2^{\parallel}$$

$$\varepsilon_1 E_1^{\perp} = \varepsilon_2 E_2^{\perp}$$

➢ for small δ, P_i values are linearly dependent

IBM **Quantum**

Analytical modeling of participation

C.E. Murray et al., IEEE TMTT **66**, 3724 (2018)

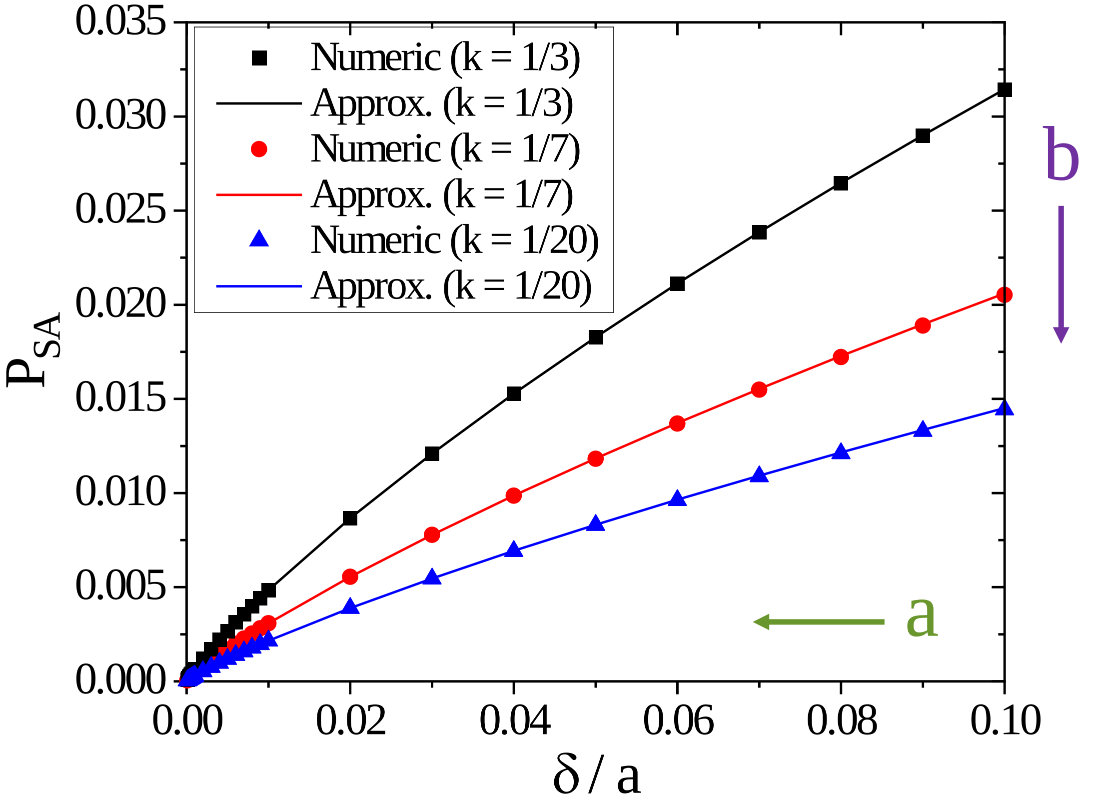

assume all $\varepsilon_C = 5.0$, $\varepsilon_{sub} = 11.45$

- $\delta \rightarrow 0$, participation $\rightarrow 0$
- nonlinear dependence vs. δ

➢ a ↑ → P_{SA} ↓ (larger gap)

➢ b ↑ (k ↓) → P_{SA} ↓ (larger paddle width)

- analytical approximation (qubits & coplanar waveguides):

$$P_{SA}\left(\frac{\delta}{a}\right) \sim \left(\frac{\epsilon_c}{\epsilon_{sub}+1}\right)\frac{1}{2(1-k)K'(k)K(k)}\left(\frac{\delta}{a}\right)\left\{\ln\left[4\left(\frac{1-k}{1+k}\right)\right]-\frac{k\ln(k)}{(1+k)}+1-\ln\left(\frac{\delta}{a}\right)\right\} \qquad k \equiv \frac{a}{b}$$

IBM **Quantum**

Results

Combine participation values with experimentally measured quality factors:

- use SA participation
- linear trend for smaller designs
  - ➢ dielectric loss dominates smaller qubit (larger participation) designs
- saturation in Q values of larger qubits
  - ➢ other mechanisms impact performance

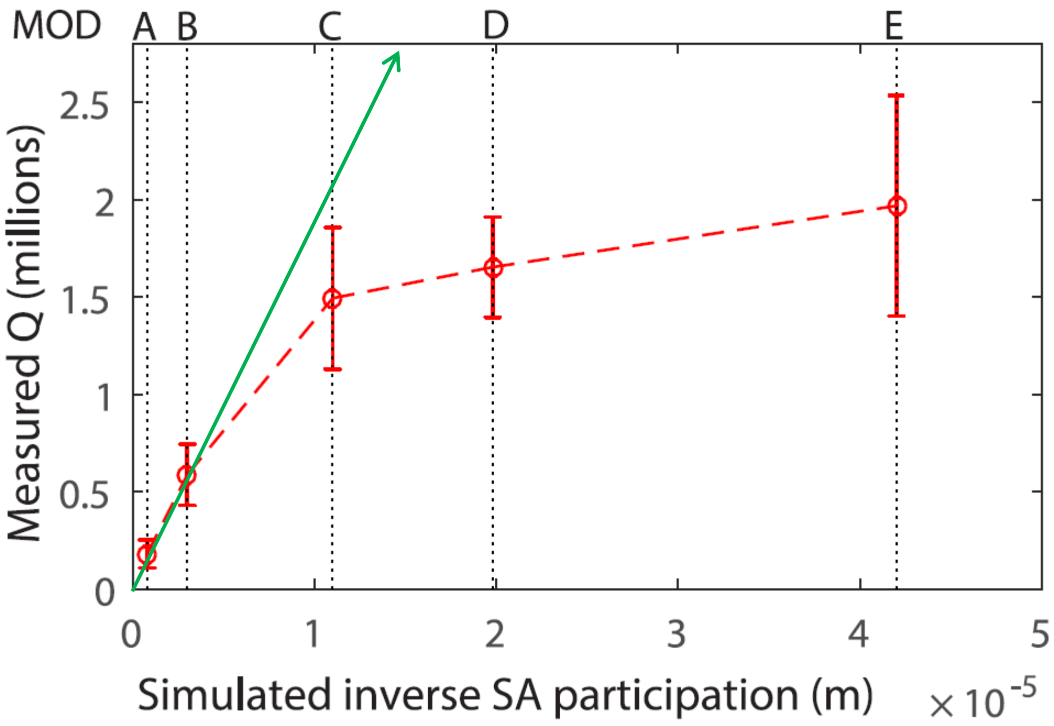

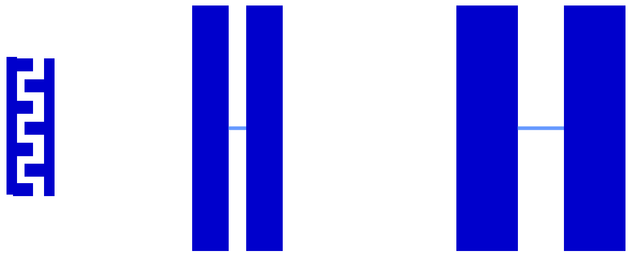

J.M. Gambetta et al., IEEE TAS **27**, 1700205 (2017)

Substrate trenching

IBM **Quantum**

- reduction in effective dielectric constant of substrate
- ➢ how is participation affected?

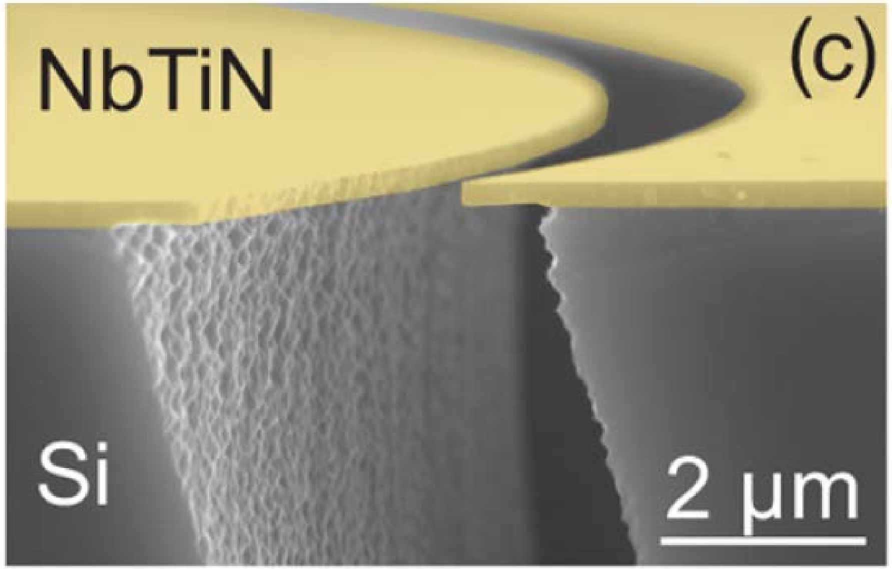

A. Bruno et al., APL**106**, 182601 (2015)

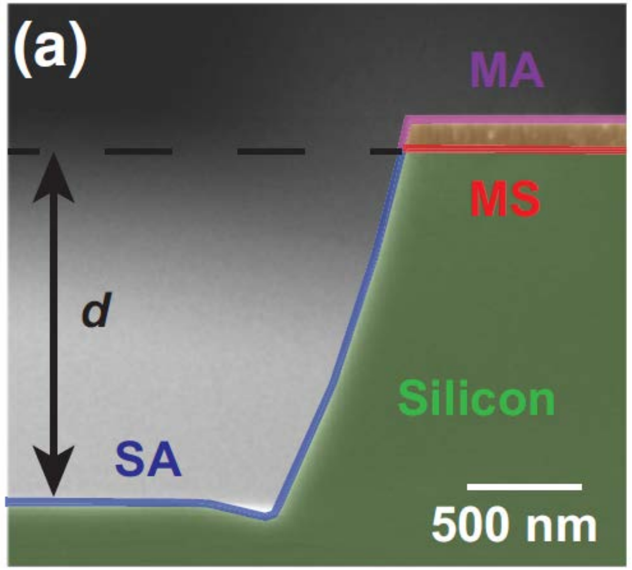

W. Woods et al., PR App. **12**, 014012 (2019)

IEEE CSC & ESAS SUPERCONDUCTIVITY NEWS FORUM (global edition), No. 49, March 2021.
Invited presentation Wk2EOr4A-04 given at the virtual ASC 2020, November 5, 2020.

Conformal mapping of trenched geometries

IBM **Quantum**

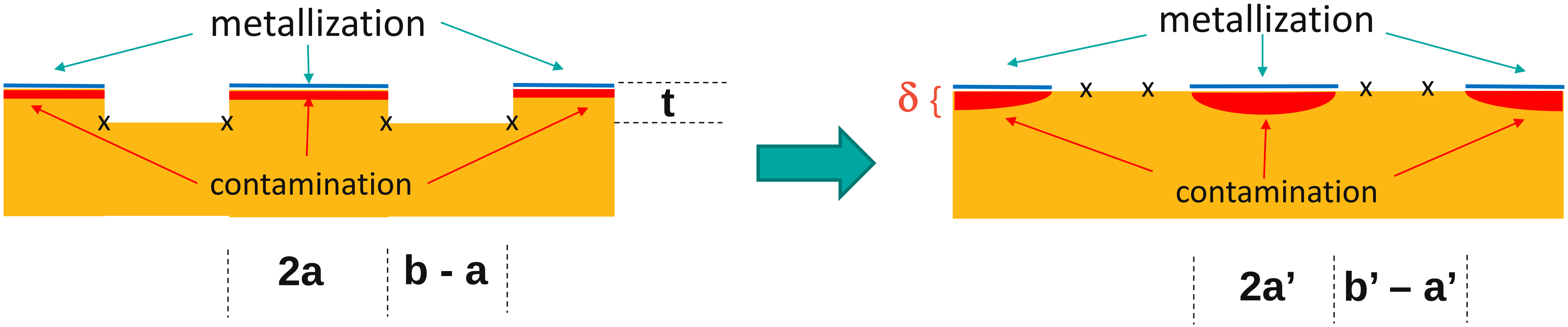

Consider CPW slice:

- assume 1D metallization
- transform trenched geometry to untrenched, half-space
- use analytical approximation of surface participation
  - ➢ transformed contamination layer thickness (δ) is no longer constant

IBM **Quantum**

Results: trenched CPW participation (2a = 10 μm, b - a = 6 μm)

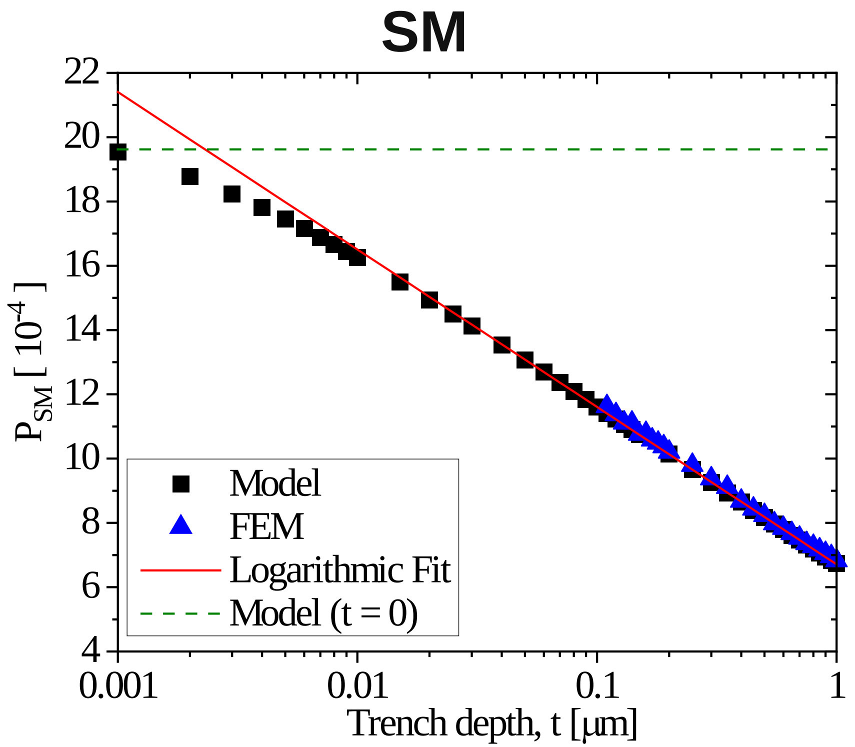

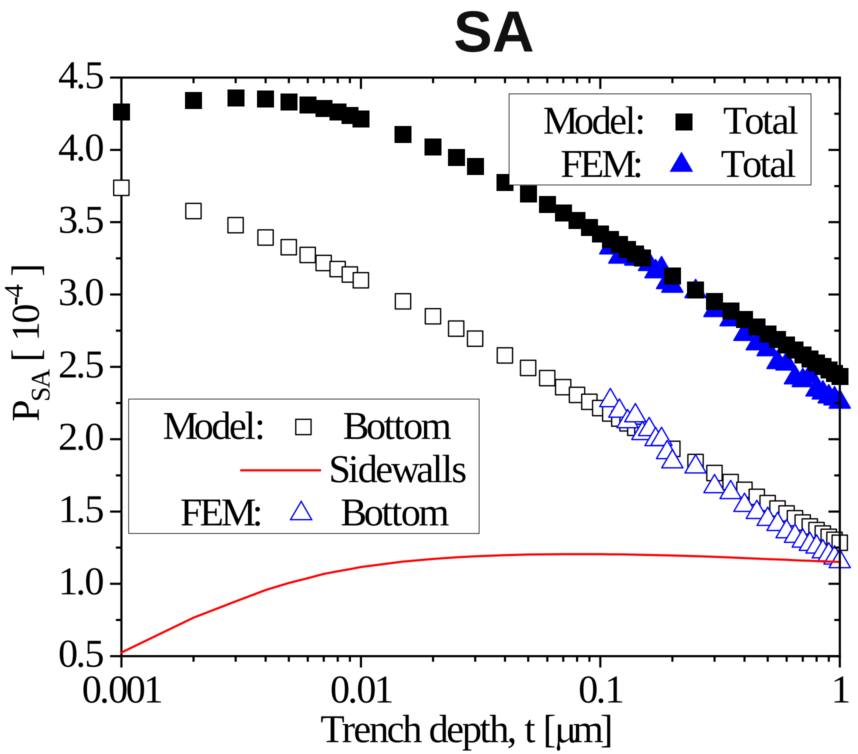

- SM participation exhibits monotonic decrease with t
- SA trench bottom participation follows SM participation
- SA sidewall contribution saturates for t > 50 nm

C.E. Murray, IEEE TMTT, **68** 3263 (2020)

Assessing dielectric loss in superconducting transmons

IBM **Quantum**

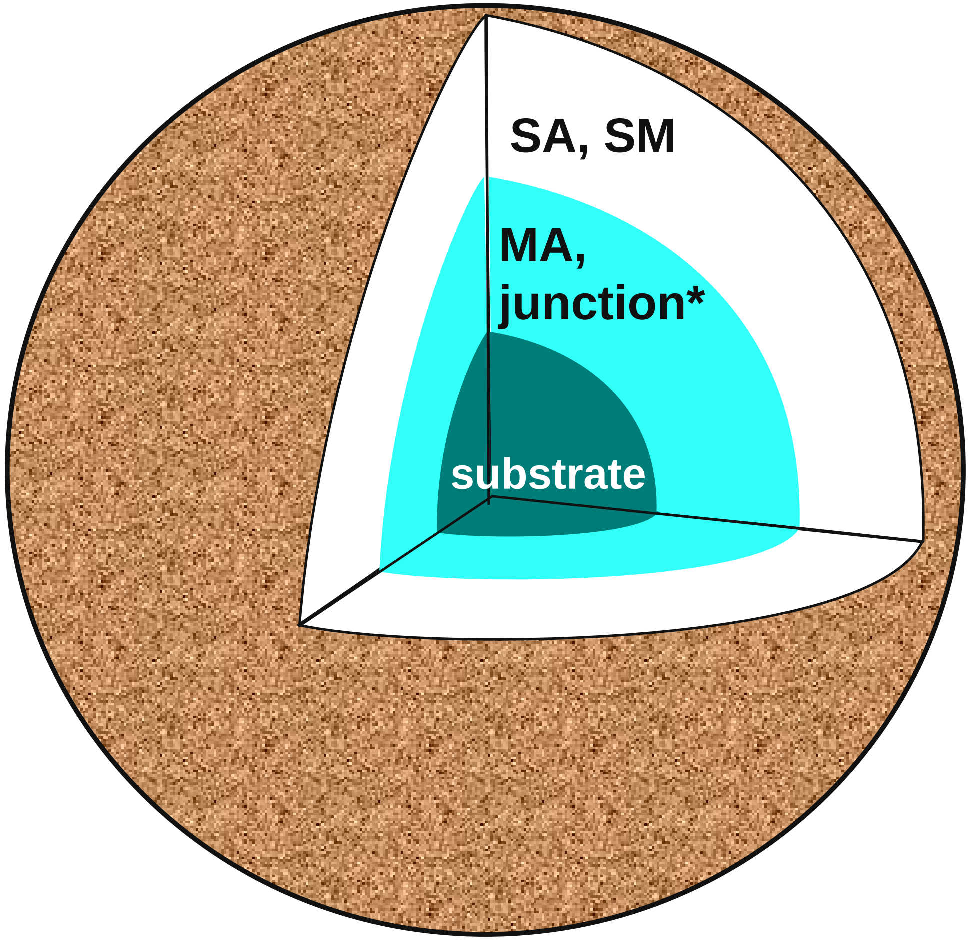

$$\frac{1}{Q_{tot}} = \sum P_i \tan(\delta_i) + \frac{1}{Q_0}$$

participation independent term

Participation (P_i):
- SA, SM ~ 10^{-4}
- MA ~ 10^{-6}
- substrate ~ 0.9

[$\varepsilon_{sub}/(\varepsilon_{sub}+1)$]

Loss Tangent:
- SA, SM ~ 10^{-3}
- MA ~ 10^{-3}
- substrate < 10^{-7}

Mitigating circumstances:
- ➢ damage, amorphization
- ➢ impurities
- * junction size

IBM **Quantum**

Implications for performance: quantum volume

metric for assessing
quantum computing performance:

- number of qubits
- gate fidelity / error rate
- circuit width
- circuit depth

A.W. Cross et al., PRA **100**, 032328 (2019)

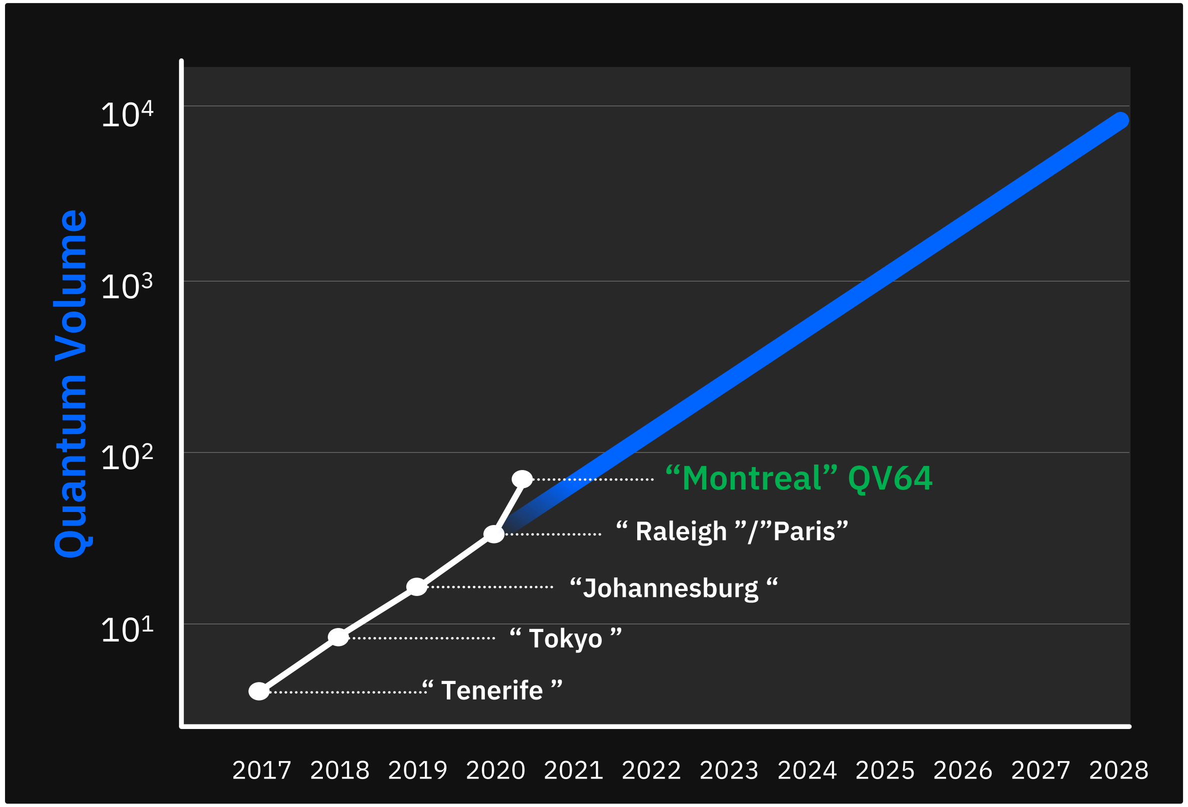

exponential trend in quantum volume growth
- doubling every year
- 2020: Montreal (27Q)

Summary and Conclusions

Superconducting quantum computing

- improvements in materials, design, processing
- reduction in relaxation due to dielectric loss

➢ search for lower-loss dielectrics

➢ identify next level of limiting mechanisms

➢ increase in quantum volume

https://www.ibm.com/quantum-computing/

Acknowledgments

- H. Paik
- M. Steffen
- M. Brink
- K. Rodbell
- J. Gambetta
- IBM Q Team

